Discoveries on the lithology of lunar crater central peaks by SELENE Spectral Profiler

Tsuneo Matsunaga,[1] Makiko Ohtake,[2] Junichi Haruyama,[2] Yoshiko Ogawa,[1]
Ryosuke Nakamura,[3] Yasuhiro Yokota,[2] Tomokatsu Morota,[2] Chikatoshi Honda,[2]
Masaya Torii,[4] Masanao Abe,[2] Tokuhiro Nimura,[2] Takahiro Hiroi,[5] Tomoko Arai,[6]
Kazuto Saiki,[7] Hiroshi Takeda,[8] Naru Hirata,[9] Shinsuke Kodama,[3] Takamitsu Sugihara,[10]
Hirohide Demura,[9] Noriaki Asada,[9] Junya Terazono,[9] and Hisashi Otake[11]

[1] The Spectral Profiler (SP) onboard the Japanese SELENE (KAGUYA) spacecraft is now providing global high spectral resolution visible-near infrared continuous reflectance spectra of the Moon. The reflectance spectra of impact craters on the farside of the Moon reveal lithologies that were not previously identified. The achievements of SP so far include: the most definite detection of crystalline iron-bearing plagioclase with its characteristic 1.3 μm absorption band on the Moon; a new interpretation of the lithology of Tsiolkovsky crater central peaks, previously classified as "olivine-rich," as mixtures of plagioclase and pyroxene; and the lower limit of Mg number of low-Ca pyroxene found at Antoniadi crater central peak and peak ring which were estimated through direct comparison with laboratory spectra of natural and synthetic pyroxene samples. **Citation:** Matsunaga, T., et al. (2008), Discoveries on the lithology of lunar crater central peaks by SELENE Spectral Profiler, *Geophys. Res. Lett.*, *35*, L23201, doi:10.1029/2008GL035868.

1. Introduction

[2] The Moon is the most intensively studied planetary body due to well-documented but limited numbers of returned samples. The synergy of the global composition constrained by remotely sensed data from previous spacecraft missions and ground truth data from returned samples and lunar meteorites has advanced our understanding of the lunar origin and evolution. For example, the five spectral bands of the US Clementine mission revealed a diverse crust stratigraphy and composition and indicated that the crust formation process was complex [*Pieters and Tompkins*, 1999a]. For more complete studies, detailed investigations of the mineralogy and lithology of the crust are necessary. Pyroxene and olivine, which are principal mafic minerals constituting the lunar crust, display charac-

teristic absorption bands at around 1 and 2 μm, associated with Fe^{2+} in the crystal structure [*Burns*, 1993], and are keys to understanding the lithology. Fe-bearing plagioclase also exhibit a broad band near 1.3 μm. Thus, the global data set of reflectance spectra across the above spectral range is really crucial for mineral identification.

[3] The Japan Aerospace Exploration Agency's (JAXA's) SELENE (Kaguya) spacecraft was launched in September 2007 and is now conducting a one-year mission observing the Moon. The optical observation system called the Lunar Imager/Spectrometer (LISM) onboard SELENE includes the Spectral Profiler (SP) [*Matsunaga et al.*, 2001], Terrain Camera (TC) [*Haruyama et al.*, 2008], and Multiband Imager (MI) [*Ohtake et al.*, 2008]. SP is a visible-near infrared spectrometer covering wavelengths from 0.5 to 2.6 μm with 296 channels with a small field of view (500 m footprint). It consists of one reflective telescope, two gratings, and three linear-array detectors. As SP global data accumulate, they will provide a powerful tool to determine the global lunar surface mineralogy and lithology. In particular, SP is the first instrument to provide continuous visible to near infrared reflectance spectra of both sides of the Moon. In this paper, we present the first scientific results of SP for the selected farside impact craters with central peaks.

2. SP Operation and Data Processing

[4] In its first six months orbiting the Moon, SP obtained pole-to-pole continuous dayside data. SP usually acquires a lunar surface spectrum every 364 msec or 550 m in the along-track direction. Due to slight time differences between exposures and the sampling interval, small gaps between measurements sometimes occur. SP data processing starts with the removal of the dark level followed by minor wavelength correction for each detector element. Preflight radiometric calibration coefficients are currently

---

[1]Center for Global Environmental Research, National Institute for Environmental Studies, Tsukuba, Japan.

[2]Institute of Space and Astronautical Science, Japan Aerospace Exploration Agency, Sagamihara, Japan.

[3]Information Technology Research Institute, National Institute of Advanced Industrial Science and Technology, Tsukuba, Japan.

[4]Fujitsu Ltd., Science Solutions Division, Sagamihara, Japan.

[5]Department of Geological Sciences, Brown University, Providence, Rhode Island, USA.

[6]Antarctic Meteorite Research Center, National Institute of Polar Research, Tokyo, Japan.

[7]Department of Earth and Space Science, Osaka University, Toyonaka, Japan.

[8]Department of Earth and Planetary Science, University of Tokyo, Tokyo, Japan.

[9]Department of Computer Software, University of Aizu, Aizu-Wakamatsu, Japan.

[10]IODP Department, Japan Agency for Marine Science and Technology, Yokohama, Japan.

[11]Lunar and Planetary Exploration Program Group, Japan Aerospace Exploration Agency, Tsukuba, Japan.
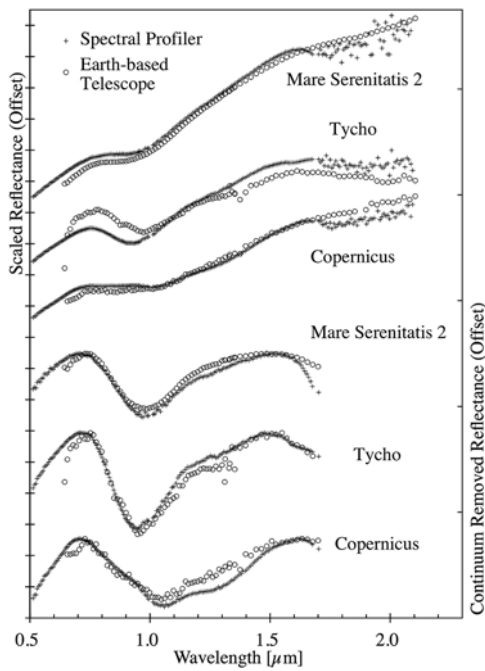
Figure 1. SP and earth-based telescopic [*Pieters and Pratt*, 2000] spectra at Mare Serenitatis-II (28.0°N, 17.5°E), and central peaks of Tycho (43.4°S, 11.1°W) and Copernicus (9.7°N, 20.1°W). (top) Reflectance spectra scaled to 1.0 at 0.75 μm and (bottom) continuum-removed spectra. No spectral or spatial averaging was applied to SP data in this and later figures. The tick intervals of vertical axes are 0.2. All spectra in this and later fiures have been vertically offset for clarity.

applied to obtain the radiance leaving the lunar surface. The stability of radiometric characteristics of SP has been monitored using internal calibration lamps.

[5] Remotely sensed lunar spectral reflectance data, such as acquired by Clementine and earth-based telescopes, were mostly calibrated against the reflectance spectra of Apollo 16 soil 62231 measured in the laboratory [*Pieters*, 1999; *Pieters and Pratt*, 2000]. The mineralogical interpretation and analysis of the lunar surface spectra greatly benefit from consistency with previous observations. Thus, SP reflectance spectra in this paper are all calibrated against the same Apollo 62231 soil. It must be noted, however, that the radiometric calibration for the longer wavelength region is still incomplete and that spectral data at wavelengths exceeding 2.2 μm are not presented in this paper. The locations of SP spectra are determined by, first, satellite position and attitude information as well as SP's line-of-sight vector data, and second, correlation analysis between SP spectra and simultaneously obtained TC or MI images.

[6] Reflectance spectra of the SP and earth-based telescopes achieve an excellent match for central peaks of Tycho and Copernicus and Mare Serenitatis (Figure 1) [*Pieters*, 1986]. Scaled SP spectra exhibit an almost monotonic increase from 0.5 to 2 μm due to space weathering [*Pieters*, 1986]. After dividing these spectra by a tangential linear continuum over the 1 μm absorption band, continuum-removed spectra of Mare Serenitatis and Tycho exhibit strong absorption features around 0.95 μm due to pyroxene,

while that of Copernicus has a broader multiple band near 1.05 μm due to olivine. These results are consistent with similar results acquired at lower resolution using earth-based telescopes [*Pieters*, 1986].

3. Plagioclase-Dominant Lithologies Observed by SP

[7] Plagioclase feldspar often has a broad absorption band around 1.3 μm. However, one of three olivine bands occurs around 1.25 μm, and Fe^{2+} in the M1 site of pyroxene yields a 1.2 μm band for both ortho- and clino-pyroxenes [*Klima et al.*, 2007a, 2007b; *Noble et al.*, 2006]. It is a complex task to distinguish the relative contribution of each when a 1.2 to 1.3 μm band is commonly accompanied with deeper 1 μm absorption as seen in Figure 1. Figure 2 contains the SP spectrum of the central peak of Jackson crater, whose continuum-removed spectrum shows a good fit to that of plagioclase measured in the laboratory with an absorption band at 1.3 μm [*Pieters and Hiroi*, 2004]. There has been a small number of lunar plagioclase spectra with a 1.3 μm band published so far [*Hawke et al.*, 1985; *Spudis et al.*, 1988; *Hawke et al.*, 2003]. Among them, a spectrum obtained on the east wall of Kant crater using an earth-based telescope shows a clearest 1.3 μm band. However, its depth (≈0.02) is much shallower than that of Jackson spectrum (≈0.1). Therefore, this SP spectrum of Jackson is the most definite detection of a crystalline 1.3 μm absorption band of iron-bearing plagioclase on the Moon obtained by both earth-based and orbital spectrometers. In contrast to Jackson, the central peak of Daedalus exhibits a linear spectrum with little 1.3 μm band. Similar spectra were found at the inner rings of large basins on the nearside [*Hawke et al.*, 2003] and at the central peaks of several nearside craters measured with low resolution telescopic spectra [*Pieters*, 1986]. The absence
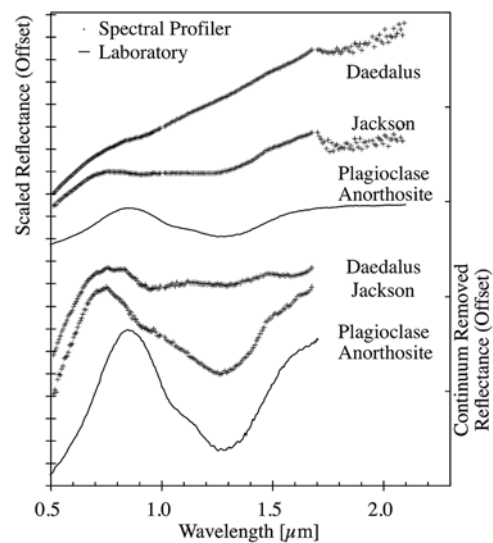
Figure 2. SP spectra of central peaks of Jackson (22.144°N, 163.085°W) and Daedalus (5.659°S, 179.464°E) craters. (top) Reflectance spectra scaled to 1.0 at 0.75 μm and (bottom) continuum-removed spectra. The laboratory spectrum of lunar anorthosite 15415 is also shown [*Pieters and Hiroi*, 2004]. The tick intervals of vertical axes of this and later figures are 0.1.
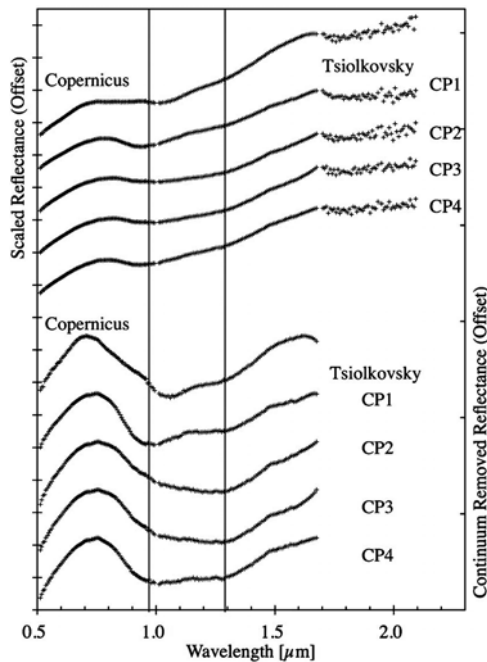
Figure 3. SP spectra of the central peaks of Tsiolkovsky crater (21.2°S, 128.9°E). (top) Reflectance spectra scaled to 1.0 at 0.75 μm and (bottom) continuum-removed spectra. The SP spectrum of Copernicus central peak is shown as a typical olivine-rich spectrum. Two vertical gray lines indicate the locations of 0.97 μm and 1.29 μm.

more spectrally active than transparent plagioclase, even a small variation of its abundance would significantly change the spectra as seen in Figure 3. In addition to Copernicus and Aristarchus studied by earth-based telescopes [*Pieters*, 1982; *Lucey et al.*, 1986], five craters were reported as possibly olivine-bearing craters based on Clementine UV/Vis images [*Pieters and Tompkins*, 1999b; *Tompkins and Pieters*, 1999]. These craters should be carefully investigated by SP to confirm the presence of olivine.

4. Low-Ca Pyroxene and Mg Number at Antoniadi

[9] A richest exposure of orthopyroxene around Antoniadi crater in the South Pole-Aitken basin (SPA) was identified using Clementine UV/Vis data [*Pieters et al.*, 2001; *Lucey*, 2004]. SP spectra of Antoniadi crater central peak and the peak ring indeed indicate a distinct shorter wavelength than that of the nearby mare basalt containing abundant high-Ca pyroxene (Figure 4). For comparison, Figure 4 also presents spectra of synthetic Mg-Fe orthopyroxene samples [*Klima et al.*, 2007a] and a natural bronzite sample from the Ogasawara Islands [*Hiroi and Pieters*, 1994]. SP spectra of the central peak and peak ring indicate very little 1.2 μm absorption band which severely limits the amount of Fe^{2+} in the M1 site of pyroxene in a similar manner to the Ogasawara sample. This indicates that pyroxenes in these locations have almost all Fe in the M2 site, which, based on band centers, limits the Fs value of their
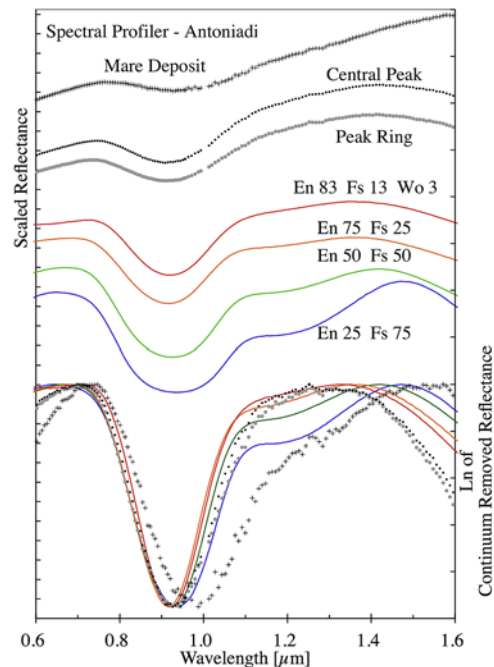
of ferrous absorption features might be explained by low FeO content below 0.1 wt% [*Adams and Goullaud*, 1978], moderate to high shock pressures which disoriented the crystal structure [*Adams et al.*, 1979; *Bruckenthal and Pieters*, 1984], optical effects due to submicroscopic iron [*Lucey*, 2002], or combinations of these. A comprehensive spectral data set is required to fully understand the relationship between the 1.3 μm absorption band and geologic conditions of plagioclase-dominated regions.

[8] Figure 3 presents another example of possible plagioclase-dominant lithology found at Tsiolkovsky. Tsiolkovsky is a conspicuous 185-km crater on the farside. The lithology of its central peak was examined using Clementine UV/Vis data [*Pieters and Tompkins*, 1999b]. Areas around the ridge crest with lower reflectance at 1 μm than those at shorter wavelengths were found and interpreted as possibly olivine-rich. However, the SP continuum-removed spectra reveal absorption bands around 0.97 and 1.3 μm at some locations within the central peaks of Tsiolkovsky, especially CP1 (Figure S1 of the auxiliary material).[1] This appears to be different from the earth-based Copernicus spectrum which exhibits characteristic olivine bands around 0.85, 1.05, and 1.25 μm. The most straightforward interpretation of the more complete SP spectra is that mixtures of plagioclase and small amounts of pyroxene of varying mixing ratios dominate the lithology for areas observed by SP although the possibility of sporadic occurrence of olivine cannot be excluded completely. Since pyroxene is

Figure 4. SP spectra of the central peak, the peak ring, and the mare deposit of Antoniadi crater (69.7S, 172.0W) in comparison with laboratory spectra of synthetic pyroxene [*Klima et al.*, 2007a] and Ogasawara bronzite [*Hiroi and Pieters*, 1994] samples. (top) Reflectance spectra scaled to 1.0 at 0.75 μm and (bottom) the natural logarithms of continuum-removed spectra scaled so as to have equal absorption depths.

pyroxene to below 50. Note that space weathering might affect the depth of 1.2 μm band also. The 1 μm band shape of these SP spectra, near its minimum at 0.93 μm, most closely resembles a synthetic pyroxene of En 50 Fs 50. These points yield a lower limit of the Mg-number (Mg#) of Antoniadi as 50. Even if the central peak contains some high-Ca pyroxene, the true 1 μm band center of the low-Ca pyroxene component would not be longer than the apparent one. Therefore, this would not change the lower limit of Mg# estimated above. Among several empirical algorithms for deriving the FeO concentration from visible-infrared spectra, a method developed by *Le Mouélic et al.* [2002] yields the best results owing to its insensitivity to topographic shading [*Lucey*, 2006]. Applying this method to Antoniadi's spectra, we calculate the FeO concentration as 15 to 16 wt% on the central peak of Antoniadi. This is much higher than the 8 to 9 wt% by the Gamma Ray Spectrometer (GRS) onboard Lunar Prospector [*Lawrence et al.*, 2002]. The discrepancy might indicate the presence of a large amount of ferroan orthopyroxene (50 < Mg# < 75) and/or olivine, which lowers the accuracy of Le Mouélic's method [*Lucey*, 2006] or target areas are too small for GRS application. Mg# higher than 50 and FeO concentration around 8 to 15 wt% indicate the presence of moderately ferroan and moderately mafic rocks. Furthermore, if Mg# > 75, which is suggested by the resemblance of SP spectra to Ogasawara bronzite and indicates less Fe in orthopyroxene, the volume fraction of orthopyroxene could be higher than those of Mg-suite rocks from the nearside. In such a case, Antoniadi's peak-ring system could be a large outcrop of the mafic-rich material rarely observed in Apollo samples and lunar meteorites. The pervasive noritic materials in the southern SPA [*Pieters et al.*, 2001] would be explained by the excavation of this low-Ca pyroxene-rich material through the SPA forming event or the subsequent impacts inside SPA. The similar spectra of the peak-ring and central peak of Antoniadi provide important constraints on the crustal structures in SPA and the formation mechanism of the peak-ring structure.

5.   Future Study

[10] Although SP is now providing new insights into lunar lithology, long-term integrated studies are required to address remaining issues such as a) the spatial distributions and origins of plagioclase with and without 1.3 μm band, b) the global distributions of "olivine-rich" areas that exhibit typical olivine spectral features and possible ultra-mafic minerals. These issues will be more fully investigated using a complete SP data set after one-year operation around the Moon. Also, the synergy with other LISM instruments, TC and MI, will significantly enhance the capability of LISM by combining detailed mineral information from SP, spatial distribution of minerals from MI, and topographic information from TC. Together with elemental composition data from gamma-ray and X-ray fluorescence spectrometers onboard SELENE and other lunar explorers, LISM data will give critical constraints on the origin and evolution of the Moon.

References

Adams, J. B., and L. H. Goullaud (1978), Plagioclase feldspar: Visible and near infrared diffuse reflectance spectra as applied to remote sensing, *Proc. Lunar Planet. Sci. Conf., 9th*, 2901–2909.

Adams, J. B., F. Horz, and R. V. Gibbons (1979), Effects of shock-loading on the reflectance spectra of plagioclase, pyroxene, and glass, *Lunar Planet. Sci. Conf., 10th*, 1–3.

Bruckenthal, E. A., and C. M. Pieters (1984), Spectral effects of natural shock on plagioclase feldspar, *Proc. Lunar Planet. Sci. Conf., 15th*, 96–97.

Burns, R. G. (1993), *Mineralogical Applications of Crystal Field Theory*, 2nd ed., 551 pp., Cambridge Univ. Press, New York.

Haruyama, J., T. Matsunaga, M. Ohtake, T. Morota, Y. Yokota, C. Honda, M. Torii, Y. Ogawa, and LISM Working Group (2008), Global lunar-surface mapping experiment using the Lunar Imager/Spectrometer on SELENE, *Earth Planets Space*, 60, 243–255.

Hawke, B. R., P. Lucey, J. F. Bell, P. Owensby, P. D. Spudis, and P. A. Davis (1985), Spectral studies of the highlands around the Nectaris basin: Preliminary results, *Proc. Lunar Planet. Sci. Conf., 16th*, 329–330.

Hawke, B. R., C. A. Peterson, D. T. Blewett, D. B. J. Bussey, P. G. Lucey, G. J. Taylor, and P. D. Spudis (2003), Distribution and modes of occurrence of lunar anorthosite, *J. Geophys. Res.*, 108(E6), 5050, doi:10.1029/2002JE001890.

Hiroi, T., and C. M. Pieters (1994), Estimation of grain sizes and mixing ratios of fine powder mixtures of common geologic minerals, *J. Geophys. Res.*, 99, 10,867–10,879.

Klima, R. L., C. M. Pieters, and M. D. Dyar (2007a), Spectroscopy of synthetic Mg-Fe pyroxenes I: Spin-allowed and spin-forbidden crystal field bands in the visible and near-infrared, *Meteorit. Planet. Sci.*, 42, 235–253.

Klima, R. L., C. M. Pieters, and M. D. Dyar (2007b), VIS-NIR spectroscopy of synthetic pyroxenes: Calcium bearing pyroxenes and application to the HED meteorites, *Lunar Planet. Sci.*, XXXVIII, Abstract 1733.

Lawrence, D. J., W. C. Feldman, R. C. Elphic, R. C. Little, T. H. Prettyman, S. Maurice, P. G. Lucey, and A. B. Binder (2002), Iron abundances on the lunar surface as measured by the Lunar Prospector gamma-ray and neutron spectrometers, *J. Geophys. Res.*, 107(E12), 5130, doi:10.1029/2001JE001530.

Le Mouélic, S., P. G. Lucey, Y. Langevin, and B. R. Hawke (2002), Calculating iron contents of lunar highland materials surrounding Tycho crater from integrated Clementine UV-visible and near-infrared data, *J. Geophys. Res.*, 107(E10), 5074, doi:10.1029/2000JE001484.

Lucey, P. G. (2002), Radiative transfer model constraints on the shock state of remotely sensed lunar anorthosites, *Geophys. Res. Lett.*, 29(10), 1486, doi:10.1029/2001GL014655.

Lucey, P. G. (2004), Mineral maps of the Moon, *Geophys. Res. Lett.*, 31, L08701, doi:10.1029/2003GL019406.

Lucey, P. G. (2006), Radiative transfer modeling of the effect of mineralogy on some empirical methods for estimating iron concentration from multi-spectral imaging of the Moon, *J. Geophys. Res.*, 111, E08003, doi:10.1029/2005JE002661.

Lucey, P. G., B. R. Hawke, C. M. Pieters, J. W. Head, and T. B. McCord (1986), A compositional study of the Aristarchus region of the Moon using near-infrared reflectance spectroscopy, *J. Geophys. Res.*, 91, D344–D354.

Matsunaga, T., M. Ohtake, Y. Hirahara, and J. Haruyama (2001), Development of a visible and near infrared spectrometer for Selenological and Engineering Explorer (SELENE), *Proc. SPIE Int. Soc. Opt. Eng.*, 4151, 32–39.

Noble, S. K., C. M. Pieters, T. Hiroi, and L. A. Taylor (2006), Using the modified Gaussian model to extract quantitative data from lunar soils, *J. Geophys. Res.*, 111, E11009, doi:10.1029/2006JE002721.

Ohtake, M., J. Haruyama, T. Matsunaga, Y. Yokota, T. Morota, C. Honda, and LISM Team (2008), Performance and scientific objectives of the SELENE (KAGUYA) Multiband Imager, *Earth Planets Space*, 60, 257–264.

Pieters, C. M. (1982), Copernicus crater central peak: Lunar mountain of unique composition, *Science*, 215, 59–61.

Pieters, C. M. (1986), Composition of the lunar highland crust from near-infrared spectroscopy, *Rev. Geophys.*, 24, 557–578.

Pieters, C. M. (1999), The Moon as a spectral calibration standard enabled by lunar samples, LPI contribution 980, paper presented at New Views of the Moon II: Understanding the Moon Through the Integration of Diverse Datasets, Lunar Planet. Inst., Flagstaff, Ariz, 22–24 Sept.

Pieters, C. M., and T. Hiroi (2004), RELAB (Reflectance Experiment Laboratory): A NASA multiuser spectroscopy facility, *Lunar Planet. Sci.*, XXXV, Abstract 1720.

Pieters, C. M., and S. Pratt (2000), Earth-based near-infrared collection of spectra for the Moon: A new PDS data set, *Lunar Planet. Sci.*, *XXXI*, Abstract 2059.

Pieters, C. M., and S. Tompkins (1999a), The distribution of lunar olivine/troctolite outcrops: Mineralogical evidence for mantle overturn?, *Lunar Planet. Sci.*, *XXX*, Abstract 2333.

Pieters, C. M., and S. Tompkins (1999b), Tsiolkovsky crater: A window into crustal processes on the lunar farside, *J. Geophys. Res.*, *104*, 21,935–21,949.

Pieters, C. M., J. W. Head III, L. Gaddis, B. Jolliff, and M. Duke (2001), Rock types of South Pole-Aitken basin and extent of basaltic volcanism, *J. Geophys. Res.*, *106*, 28,001–28,022.

Spudis, P. D., B. R. Hawke, and P. G. Lucey (1988), Geology and deposits of the lunar Nectaris basin, *Lunar Planet. Sci.*, *XIX*, Abstract 1115.

Tompkins, S., and C. M. Pieters (1999), Mineralogy of the lunar crust: Results from Clementine, *Meteorit. Planet. Sci.*, *34*, 25–41.

M. Abe, J. Haruyama, C. Honda, T. Morota, T. Nimura, M. Ohtake, and Y. Yokota, Institute of Space and Astronautical Science, Japan Aerospace Exploration Agency, 3-1-1 Yoshinodai, Sagamihara, Kanagawa 229-8510, Japan.

T. Arai, Antarctic Meteorite Research Center, National Institute of Polar Research, 1-9-10 Kaga, Itabashi, Tokyo 173-8515, Japan.

N. Asada, H. Demura, N. Hirata, and J. Terazono, Department of Computer Software, University of Aizu, Ikki-machi, Aizu-Wakamatsu, Fukushima 965-8580, Japan.

T. Hiroi, Department of Geological Sciences, Brown University, 324 Brook Street, Providence, RI 02912, USA.

S. Kodama and R. Nakamura, Information Technology Research Institute, National Institute of Advanced Industrial Science and Technology, 1-1-1 Umezono, Tsukuba, Ibaraki 305-8568, Japan.

T. Matsunaga and Y. Ogawa, Center for Global Environmental Research, National Institute for Environmental Studies, 16-2 Onogawa, Tsukuba, Ibaraki 305-8506, Japan. (matsunag@nies.go.jp)

H. Otake, Lunar and Planetary Exploration Program Group, Japan Aerospace Exploration Agency, 2-1-1 Sengen, Tsukuba, Ibaraki 305-8505, Japan.

K. Saiki, Department of Earth and Space Science, Osaka University, 1-1 Machikaneyama, Toyonaka, Osaka 560-0043, Japan.

T. Sugihara, IODP Department, Japan Agency for Marine Science and Technology, Showa-machi 3173-25, Kanazawa-ku, Yokohama, Kanagawa 236-0001, Japan.

H. Takeda, Department of Earth and Planetary Science, University of Tokyo, 7-3-1 Hongo, Bunkyo, Tokyo 113-0033, Japan.

M. Torii, Fujitsu Ltd., Science Solutions Divisions, 3-1-1 Yoshinodai, Sagamihara, Kanagawa 229-8510, Japan.